Biochemical and Biophysical Research Communications 434 (2013) 60–64

Contents lists available at SciVerse ScienceDirect

Biochemical and Biophysical Research Communications

journal homepage: www.elsevier.com/locate/ybbrc

Analysis of ischemic neuronal injury in $Ca_V2.1$ channel α_1 subunit mutant mice

Xiaoli Tian [a,1], Ying Zhou [b,1], Linghan Gao [b], Guang He [b], Weizhong Jiang [c], Weidong Li [b], Eiki Takahashi [b,d,*]

[a] Division of Pulmonary and Critical Care Medicine, David Geffen School of Medicine, University of California, Los Angeles, CA 90095-1690, USA
[b] Bio-X Institutes, Key Laboratory for the Genetics of Developmental and Neuropsychiatric Disorders (Ministry of Education), Shanghai Jiao Tong University, Shanghai 200240, PR China
[c] Department of Neurosurgery, The Fifth People's Hospital of Shanghai, Fudan University, Shanghai 200240, PR China
[d] Research Resources Center, RIKEN Brain Science Institute, Saitama 351-0198, Japan

ARTICLE INFO

Article history:
Received 6 March 2013
Available online 29 March 2013

Keywords:
$Ca_V2.1$
Ca^{2+} imaging
Ischemic neuronal injury
Leaner mice
Middle cerebral artery occlusion
Rolling Nagoya mice

ABSTRACT

One of the main instigators leading to cell death and brain damage following ischemia is Ca^{2+} dysregulation. Neuronal membrane depolarization results in the activation of voltage-gated Ca^{2+} (Ca_V) channels and intracellular Ca^{2+} influx. We investigated the physiological role of the $Ca_V2.1$ (P/Q-type) channel in ischemic neuronal injury using $Ca_V2.1$ channel α_1 subunit mutant mice, *rolling Nagoya* and *leaner mice*. The *in vivo* ischemia model with a complete occlusion of the middle cerebral artery showed that the infarct area at 24 h was significantly smaller in *rolling Nagoya* (27.1 ± 3.5% of total brain volume) and *leaner* (20.1 ± 3.5%) mice compared to wild-type (42.9 ± 4.5%) mice. In an *in vitro* Ca^{2+} imaging study, oxygen–glucose deprivation using a hippocampal slice induced a significantly slower rate of increase in intracellular Ca^{2+} concentration ($[Ca^{2+}]i$) in *rolling Nagoya* (0.083 ± 0.007/min) and *leaner* (0.062 ± 0.006/min) mice compared to wild-type (0.105 ± 0.008/min) mice. These results demonstrate that the mutant $Ca_V2.1$ channel in *rolling Nagoya* and *leaner* mice plays a different protective role in a ($[Ca^{2+}]i$)-dependent manner in ischemic models and indicate that $Ca_V2.1$ channel blockers may be used preventively against ischemic injury.

1. Introduction

Voltage-gated Ca^{2+} (Ca_V) channels allow the entry of Ca^{2+} into a cell when the membrane is depolarized. In the nervous system, Ca_V channels play an important role in regulating diverse neuronal functions attributed to elevated intracellular Ca^{2+} concentrations ($[Ca^{2+}]i$) [1]. The Ca_V channel is a molecular complex consisting of α_1, β, α_2-δ, and γ subunits [2]. The α_1 subunit is essential for proper channel function and determines the fundamental properties of the channel [1]. At the presynaptic terminal, three major Ca_V2 channel types, $Ca_V2.1$ (P/Q-type), $Ca_V2.2$ (N-type), and $Ca_V2.3$ (R-type), are broadly expressed in the central nervous system [3] and are involved in the Ca^{2+}-dependent exocytotic release of neurotransmitters [4]. Given the pivotal role of Ca_V2 channels in controlling specific neurotransmitter production and release, defects in the expression, localization, structure, or modulation of presynaptic Ca_V2 channels may result in aberrant synaptic signaling, leading to various patterns of neural network dysfunction.

An increase in $[Ca^{2+}]i$ plays an essential role in the pathogenesis of ischemic neuronal injury [5–8]. The $[Ca^{2+}]i$ is elevated in ischemia via both Ca^{2+} influx from the extracellular space and Ca^{2+} release from the intracellular store [9]. Because the Ca_V2 channels are important as a Ca^{2+} influx route, their involvement in the pathophysiology of ischemic neuronal injury is crucial.

To examine $Ca_V2.1$ channel functions and disease processes among Ca_V2 channels, genetic studies of mice can be useful. Mice with mutations in the *Cacna1a* gene encoding the pore-forming α1 subunit of $Ca_V2.1$ channels include the knockout strain lacking $Ca_V2.1$ currents and spontaneous strain including *rolling Nagoya* and *leaner* mice exhibiting ataxia as a common symptom [10–12]. The *rolling Nagoya* mice have a mutation in the voltage-sensing S4 segment of the third repeat [13], and *leaner* mice have a mutation in a splice donor consensus sequence, which results in altered C-terminal sequences [14]. The *rolling Nagoya* mutant $Ca_V2.1$ channel has lowered voltage sensitivity of activation leading to impaired synaptic transmission in the cerebellum [15]. The *leaner* mutant $Ca_V2.1$ channel results in low expression density of the channels in the cerebellum [16]. Previous studies have also shown that the reduction in P-type Ca^{2+} currents is greater in the Purkinje cells of *leaner* mice (60%) than in *rolling Nagoya* mice (40%) [13,16]. Using $Ca_V2.1$ channel α_1 subunit ($Ca_V2.1\alpha_1$) knockout mice to examine the relationship between $Ca_V2.1$ channel and ischemic neuronal injury is impossible because most of the mice do not sur-

* Corresponding author. Address: Research Resources Center, RIKEN Brain Science Institute, 2-1 Hirosawa, Wako, Saitama 351-0198, Japan. Fax: +81 48 467 9692.
E-mail address: etakahashi@brain.riken.jp (E. Takahashi).
[1] These authors contributed equally to this work.

0006-291X/$ - see front matter © 2013 Elsevier Inc. All rights reserved.
http://dx.doi.org/10.1016/j.bbrc.2013.03.066

vive past weaning. Although *rolling Nagoya* and *leaner* mice exhibit a normal life span, the severity of ataxia differs significantly, being more severe in *leaner* mice than in *rolling Nagoya* mice. Because the precise regulation of Ca^{2+} signaling is important for neuronal processes, changes in Ca^{2+} currents through different mutant $Ca_V2.1$ channels induce different dysfunctions of neurons and circuits. Thus, a comparison of *rolling Nagoya* and *leaner* mice and wild-type mice could elucidate the physiological role of the $Ca_V2.1$ channel in ischemic neuronal injury.

In the present study, we investigated the role of the $Ca_V2.1$ channel in ischemic neuronal injury using an *in vivo* ischemia model with complete occlusion of the middle cerebral artery (MCA) and an *in vitro* ischemia model with oxygen–glucose deprivation (OGD) in a hippocampal slice using *rolling Nagoya* and *leaner* mice.

2. Materials and methods

2.1. Animals

All animal procedures were approved by the Animal Experiments Committee of Shanghai Jiao Tong University and RIKEN, and were conducted in accordance with the Institutional Guidelines for Experiments using Animals. The *rolling Nagoya* mouse strain was provided by the RIKEN BioResource Center with the support of the National BioResource Project of the Ministry of Education, Culture, Sports, Science, and Technology of Japan and backcrossed to C57BL/6J mice for 14 generations. The *leaner* mouse strain with the C57BL/6J genetic background was provided by the Jackson Laboratory. The mice were given free access to water and food pellets (CRF-1, Oriental Yeast Co., Ltd., Tokyo, Japan) and were housed under a 12/12-h light/dark cycle (lights on from 08:00 to 20:00) at 23 ± 1 °C and 55 ± 5% humidity. All analyses were conducted by a well-trained experimenter who was blinded to the mouse genotypes.

2.2. In situ hybridization

Paraffin-embedded blocks and sections of brains from 16-week-old male mice for *in situ* hybridization (ISH) were obtained from Genostaff Co., Ltd. (Tokyo, Japan). Each mouse brain was dissected after perfusion, fixed with Tissue Fixative (Genostaff), then embedded in paraffin according to proprietary procedures and sectioned at 6 μm. The hybridization protocol was conducted as previously reported [17]. The probe for a 691 bp cDNA fragment was designed from positions 6068 to 6748 of the $Ca_V2.1\alpha_1$ subunit cDNA and labeled with digoxygenin RNA labeling kit (Roche Diagnostics, Mannhein, Germany). Coloring reactions were performed with NBT/BCIP solution (Sigma–Aldrich, St. Louis, MO, USA) overnight and then washed with PBS. The sections were counterstained with Kernechtrot stain solution (Mutoh Pure Chemicals, Tokyo, Japan) and mounted with CC/Mount (Diagnostic Biosystems Inc., Pleasanton, CA, USA).

2.3. Real-time quantitative reverse transcription polymerase chain reaction

Total RNA was isolated from the olfactory bulb, cerebral cortex, caudate putamen, hippocampus, cerebellum, and liver of 16-week-old male mice using TRIzol reagent, according to the manufacturer's protocol (Invitrogen, Carlsbad, CA, USA). To quantify the mRNA level of the gene of interest, we employed real-time quantitative reverse transcription polymerase chain reaction (qRT-PCR) using an ABI7700 sequence detection system (Applied Biosystems, Foster City, CA, USA) as previously reported [18]. To determine the total amount of both wild-type and mutant $Ca_v2.1\alpha_1$ gene expression, the primers used were CT1F (5′-CTGCGCTACTTCGAGATGTG-3′) and CT1R (5′-AACATAGTCAAAATATCGCAGCAC-3′), and the probe was MT-probe1 (5′-ATCCTCATGGTCATTGCCATGAGCAG-CATCGCTCTGGCCGCCGAGGACCCGGTGCAGCCCAACGCACCCC-3′). To confirm equivalent loading, the amount of 18S ribosomal RNA in each sample was determined using standard primers and TaqMan probes (Applied Biosystems). All samples were analyzed in duplicate and average values were used for the relative quantification of gene expression. All samples were analyzed in duplicate. The mRNA expression level was calculated relative to $Ca_v2.1\alpha_1$ mRNA expression in wild-type mice.

2.4. MCA occlusion

In vivo ischemia was induced by the MCA occlusion method as described previously [19]. The 16-week-old male mice were anesthetized using isoflurane and body temperature was maintained (36 ± 0.5 °C) using a water-jacketed heating pad. The skin was incised, and the left occipital and superior thyroid artery, branches of the external carotid artery (ECA), as well as the pterygopalatine artery were exposed, electrocoagulated, and cut. After occlusion of the common carotid artery by microclip, the left ECA was ligated, coagulated, and cut distally to the cranial thyroid artery. A 21-mm monofilament nylon suture (5–0, Harvard Apparatus, Holliston, MA, USA; diameter of the heat-rounded tip: 0.2–0.3 mm) was inserted into the ECA and gently advanced through the internal carotid artery until its tip occluded the origin of the MCA. Correct placement of the suture was confirmed by a sudden drop of the local cortical blood flow in the left MCA territory to 10–15% of basal flow as monitored by laser-Doppler flowmetry. After successful occlusion, the monofilament was secured in place with ligature, and the skin incision was closed by surgical clips.

2.5. Evaluation of infarct size

Twenty-four hours after MCA occlusion, mice were anesthetized with an overdose of pentobarbital sodium and decapitated. Brains were removed and were serially sectioned into five coronal slices (1 mm thick) with a vibratome (VT1000S, Leica Microsystems, Wetzlar, Germany). The sections were immersed in 1% 2,3,5-triphenyltetrazolium chloride (TTC) in saline and incubated for 30 min at 37 °C. Infarct images and the entire contralateral hemisphere were captured using a digital camera and areas were measured using Image software (Win ROOF Version 5.7, MITANI Corporation, Tokyo, Japan). The infarct area was determined by subtracting the area of the non-infarcted ipsilateral hemisphere from the contralateral tissue. The percentage of infarct volume was calculated by dividing the sum of the area of infarction by the total contralateral hemisphere as described previously [20].

2.6. Ca^{2+} imaging in oxygen–glucose deprived hippocampal slices

In vitro ischemia was induced as described previously [21]. Hippocampal slices (350 μm) were made from 5-week-old male mice using a vibratome (VT1000S, Leica Microsystems) and placed in ice-cold artificial cerebrospinal fluid (ACSF). The ACSF was composed of 137 mM NaCl, 2.5 mM KCl, 21 mM $NaHCO_3$, 0.58 mM NaH_2PO_4, 2.5 mM $CaCl_2$, 1.2 mM $MgCl_2$ and 10 mM glucose, and the pH was 7.4 under saturation with 95% O_2/5% CO_2. After 2 h incubation, the slices were stained with the fluorescent Ca^{2+} indicator Fura-PE3/AM (10 μM, Calbiochem, San Diego, CA, USA) and 0.01% Cremophor EL (Sigma–Aldrich) for 45 min at 37 °C. Then the slices were thoroughly washed for 30 min to remove any extracellular dye. The slices were superfused (4 mL/min) at 35 °C on a stage of an inverted epifluorescence microscope (TMD-300, Nikon

Corporation, Tokyo, Japan) and were alternately excited at 340 and 380 nm wavelengths to capture fluorescence signals (F340 and F380) every 1 min (Argus50, Hamamatsu Photonics, Shizuoka, Japan). The $[Ca^{2+}]$i in CA1 was estimated by mean values of the fluorescence ratio (ratio = F340/F380) from two different regions of the CA1 stratum pyramidale. To apply OGD, ACSF was saturated with 95% N_2/5% CO_2 and glucose was replaced by 2-deoxy-D-glucose (10 mM). To standardize a temporal profile of $[Ca^{2+}]$i increase during OGD, a normalized ratio was calculated by dividing each obtained ratio by the baseline ratio (the average of five values before application of OGD). Then the maximal rate of increase in the normalized ratio was calculated using running bins in 3-min intervals.

2.7. Statistical analysis

Data are presented as means ± standard error of the mean (SEM). Statistical analyses for the behavioral and immunocytochemical studies were conducted using Excel Statistics 2006 (SSRI, Tokyo, Japan). Data were analyzed using repeated measures analysis of variance (ANOVA) followed by Tukey's post hoc tests.

3. Results

3.1. Expression patterns of $Ca_v2.1\alpha_1$ mRNA

We performed ISH to assess the localization of $Ca_V2.1\alpha_1$ mRNA in wild-type ($n = 6$), *rolling Nagoya* ($n = 5$), and *leaner* mice ($n = 5$); they were the same (data not shown). Using the antisense probe, all three mice strains showed a broad expression of the α_1 subunit in the brain with strong expression in the olfactory bulb, cerebral cortex, hippocampus, and cerebellar Purkinje cells. There were no signals in any of the brains using the sense probe. To expression levels of $Ca_V2.1\alpha_1$ mRNA in the olfactory bulb, cerebral cortex, caudate putamen, hippocampus, cerebellum, and liver of the three types of mice ($n = 10$ for each group), we used real-time qRT-PCR analysis. The relative expression level of total $Ca_V2.1\alpha_1$ was not significantly different among the strains in the olfactory bulb [wild-type, *rolling Nagoya*, and *leaner*: 1.01 ± 0.04, 1.03 ± 0.06, and 1.04 ± 0.07, respectively; $F(2,27) = 0.153$, $p > 0.05$], cerebral cortex [wild-type, *rolling Nagoya*, and *leaner*: 1.03 ± 0.01, 1.03 ± 0.04, and 1.04 ± 0.08, respectively; $F(2,27) = 0.173$, $p > 0.05$], caudate putamen [wild-type, *rolling Nagoya*, and *leaner*: 1.02 ± 0.05, 1.03 ± 0.03, and 1.04 ± 0.04, respectively; $F(2,27) = 0.145$, $p > 0.05$], hippocampus [wild-type, *rolling Nagoya*, and *leaner*: 1.02 ± 0.01, 1.05 ± 0.08, and 1.02 ± 0.07, respectively; $F(2,27) = 0.166$, $p > 0.05$], and cerebellum [wild-type, *rolling Nagoya*, and *leaner*: 1.02 ± 0.02, 1.03 ± 0.03, and 1.06 ± 0.03, respectively; $F(2,27) = 0.182$, $p > 0.05$]. The liver fraction did not yield a detectable PCR product in any of the strains (data not shown).

3.2. Decreased stroke volume in $Ca_V2.1\alpha_1$ gene mutant mice in an in vivo ischemia model

The wild-type ($n = 12$), *rolling Nagoya* ($n = 11$), and *leaner* ($n = 12$) mice were subjected to MCA occlusion. The infarct was identified as an unstrained (white) area surrounded by strained (red) viable tissue. Fig. 1A shows a representative experiment in which infarct areas were stained 24 h after permanent occlusion with TTC. The MCA occlusion resulted in significantly different infarct areas among the three mice strains [$F(2,32) = 98.152$, $p < 0.01$]. The infarct area after stroke was 27.1 ± 3.5% of total brain volume in *rolling Nagoya* mice ($p < 0.01$) and 20.2 ± 3.5% of total brain volume in *leaner* mice ($p < 0.01$) compared to 42.9 ± 4.5% in wild-type mice (Fig. 1B).

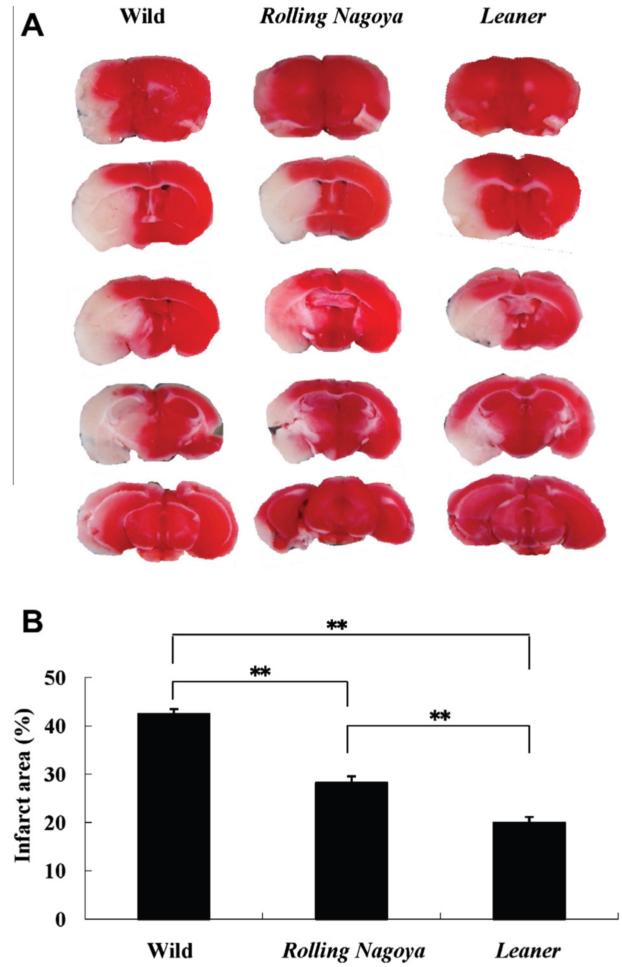

Fig. 1. Evaluation of cerebral infarction. (A) Serial brain sections after middle cerebral artery (MCA) occlusion. Representative 2,3,5-triphenyltetrazolium chloride (TTC) staining of brain sections from wild-type (left lane), *rolling Nagoya* (middle lane), and *leaner* (right lane) mice. (B) Quantification of the volume of the ischemic lesion in wild-type ($n = 12$), *rolling Nagoya* ($n = 11$), and *leaner* ($n = 12$) mice. $^{**}p < 0.01$, compared to the appropriate control (Tukey's test).

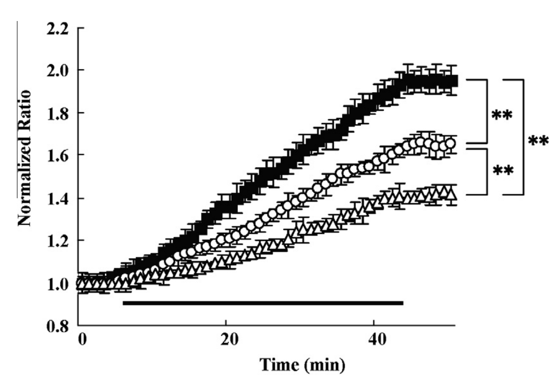

Fig. 2. Profiles of the $[Ca^{2+}]$i increase induced by oxygen–glucose deprivation (OGD) in hippocampal slices. Time courses of changes in the normalized ratio induced by OGD in the pyramidal cell layer of the hippocampal CA1 region from wild-type ($n = 14$, closed square), *rolling Nagoya* ($n = 14$, open circle), and *leaner* ($n = 14$, open triangle) mice. Normalized ratios are plotted against time from 5 min before the start of OGD to 7 min after the end of OGD. Horizontal black bars indicate the treatment with OGD. $^{**}p < 0.01$, compared to the appropriate control (Tukey's test).

3.3. Decreased [Ca2+]i in $Ca_V2.1\alpha_1$ gene mutant mice in an in vitro ischemia model

To investigate whether the decreased infarct volume in mutant mice was related to neuronal Ca^{2+} signaling, we examined the changes in $[Ca^{2+}]$i induced by OGD, an ischemia-like condition, using a hippocampal slice preparation. The $Ca_V2.1$ channel was strongly expressed in the hippocampal region. Before the application of OGD, there were no significant differences observed among the three mice strains in the basal ratio of the CA1 pyramidal cell layer (wild-type mice: 0.847 ± 0.011, *rolling Nagoya* mice: 0.827 ± 0.022, *leaner* mice: 0.803 ± 0.013). After the start of the OGD treatment there was a progressive increase in $[Ca^{2+}]$i in the strains, and the normalized ratio from 4 min after the start was significantly higher in wild-type mice than in *rolling Nagoya* and *leaner* mice (Fig. 2). The maximal rate of increase was significantly different among the three mice strains [$F(98,1950) = 4.712$, $p < 0.01$]. The rate was 0.083 ± 0.007/min in the *rolling Nagoya* mice ($p < 0.01$) and 0.062 ± 0.006/min in the *leaner* mice ($p < 0.01$) compared to 0.105 ± 0.008/min in the wild-type mice.

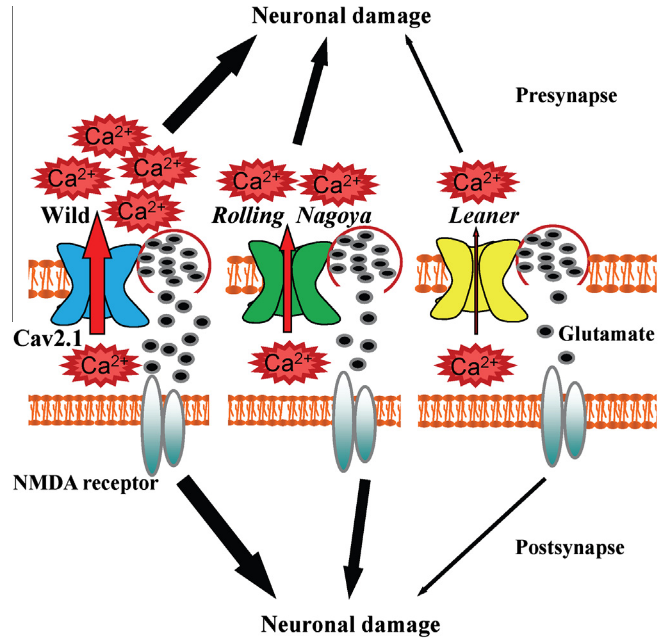

Fig. 3. Putative mechanism for mutant $Ca_V2.1$ channel mediated neuroprotection in the ischemia stage. The $Ca_V2.1$ channels are important as a Ca^{2+} influx route and regulate glutamate release. An increase in $[Ca^{2+}]$i plays an essential role in the pathogenesis of ischemic neuronal injury. During ischemia, different mutant $Ca_V2.1$ channels influence different Ca^{2+} currents and glutamate releases, leading to neuronal damage.

4. Discussion

Although $Ca_V2.2\alpha_1$ and $Ca_V2.3\alpha_1$ gene knockout mice have a normal life span [22], $Ca_V2.1\alpha_1$-deficient mice die 3–4 weeks after birth [23]. Among the predominantly neuronal Ca_V2 channel family, which includes $Ca_V2.1$, $Ca_V2.2$, and $Ca_V2.3$, the $Ca_V2.1$ channel appears to be indispensable, suggesting that its involvement in the pathophysiology of neuronal injury is crucial. The $Ca_V2.1\alpha_1$ gene is broadly expressed in the brain including the cerebral cortex, caudate putamen, and hippocampus [14]. In MCA occlusion, the caudate putamen becomes an ischemic core and the cerebral cortex comprises the ischemic penumbra area.

We first examined the expression patterns of the mutant $Ca_V2.1\alpha_1$ gene in the brain from *rolling Nagoya* and *leaner* mice. ISH studies showed no apparent cells with different expression in the brain among *rolling Nagoya*, *leaner*, and wild-type mice. Then, we examined the expression levels of the mutant $Ca_V2.1\alpha_1$ gene in the olfactory bulb, cerebral cortex, caudate putamen, hippocampus, and cerebellum of *rolling Nagoya*, *leaner*, and wild-type mice. There were no significantly different levels in these sites among them.

Excessive intracellular Ca^{2+} influx is a major instigator of neuronal cell death following cerebral ischemia. The Ca^{2+} influx is mediated by a number of important channels and transporters. The $Ca_V2.1$ channel plays an important role in physiological neurotransmitter release from mammalian nerve terminals via the influx of Ca^{2+} after depolarization [1], but its involvement under pathological conditions is not clearly understood. In this study, to address the involvement of the $Ca_V2.1$ channel in ischemic brain injury, we evaluated the effects of brain injury in *rolling Nagoya* and *leaner* mice using *in vivo* and *in vitro* ischemia models. The results showed significant protective effects in both models in both strains. The infarct volumes 24 h after MCA occlusion were 36.4% and 53.2% lower in *rolling Nagoya* and *leaner* mice, respectively, than wild-type mice. In Ca^{2+} imaging experiments using hippocampal slice preparations, OGD-induced $[Ca^{2+}]$i showed a slower increase in mutant mice than in wild-type mice. The rate of increase in $[Ca^{2+}]$i was slower in *leaner* mice than in *rolling Nagoya* mice. The focal ischemia model used in the present study usually forms a predominantly ischemic core and mildly ischemic peripheral penumbra areas. In the ischemia stage, $[Ca^{2+}]$i in penumbra neurons triggers a Ca^{2+}-mediated intracellular signaling cascade near the threshold level, leading to ischemic neuronal death. Accordingly, the weakened rate of increase in Ca^{2+} could critically influence the degree of penumbra neurons leading to less cell death in $Ca_V2.1$ mutant mice. During ischemia, Ca^{2+}-dependent exocytotic glutamates are released from nerve terminals [24,25] and Ca^{2+}-independent release mediates reversal glutamate transporter from nerve terminals or glial cells [26,27]. Ischemic neuronal damage is exacerbated by the action of N-methyl-D-aspartate (NMDA) receptors [28]. A previous study demonstrated that gene disruption of the NR2C subunit of the NMDA receptor attenuates focal cerebral ischemic injury after permanent MCA occlusion [29]. In addition, physiological glutamatergic synaptic transmission is regulated by Ca^{2+}-dependent glutamate release regulated by the $Ca_V2.1$ channel [30], suggesting that the ischemic protective results observed in our study may be produced by the attenuation of the extracellular glutamate due to Ca^{2+}-dependent exocytotic release coupled to the mutant $Ca_V2.1$ channel, although we have not confirmed the presence of glutamate release dysfunctions in *rolling Nagoya* and *leaner* mice. Fig. 3 shows a schematic diagram on the hypothetical mechanisms for mutant $Ca_V2.1$ channel mediated neuroprotection in the ischemia stage.

In the present study, we demonstrated that mutation of the gene for the α_1 subunit of the $Ca_V2.1$ channel in *rolling Nagoya* and *leaner* mice protects the brain from ischemic injury. Our results show that different $Ca_V2.1\alpha_1$ gene allelic variants exhibit considerable variability in phenotypes. Thus, a detailed comparison of allelic variants may be helpful for clarifying the relationships among the many different biophysical and structural synaptic abnormalities and observed behavioral deficits.

Acknowledgments

This work was supported by the China 973 project (2010CB529604), National Scientific Foundation of China (81271511 and 30900432), Program for Professor of Special Appointment (Eastern Scholar) at Shanghai Institutions of Higher Learning, "Shu Guang" Project supported by Shanghai Municipal

Education Commission and Shanghai Education Development Foundation, Shanghai Pujiang Program to WL and Grants-in-Aid for Scientific Research KAKENHI (22500396) to ET. The authors reported no biomedical financial interests or potential conflicts of interest.

References

[1] W.A. Catterall, A.P. Few, Ca^{2+} channel regulation and presynaptic plasticity, Neuron 59 (2008) 882–901.
[2] W.A. Catterall, Structure and function of neuronal Ca^{2+} channels and their role in neurotransmitter release, Cell Calcium 24 (1998) 307–323.
[3] O. Tanaka, H. Sakagami, H. Kondo, Localization of mRNAs of voltage-dependent Ca^{2+} channels: four subtypes of alpha 1- and beta-subunits in developing and mature rat brain, Brain Res. Mol. Brain Res. 30 (1995) 1–16.
[4] W.A. Catterall, Interactions of presynaptic Ca^{2+} channels and snare proteins in neurotransmitter release, Ann. NY Acad. Sci. 868 (1999) 144–159.
[5] D.W. Choi, Ionic dependence of glutamate neurotoxicity, J. Neurosci. 7 (1987) 369–379.
[6] J.L. Cross, B.P. Meloni, A.J. Bakker, S. Lee, N.W. Knuckey, Modes of neuronal calcium entry and homeostasis following cerebral ischemia, Stroke Res. Treat. (2010) 316862.
[7] M.P. Mattson, R.J. Mark, Excitotoxicity and excitoprotection *in vitro*, Adv. Neurol. 71 (1996) 1–30.
[8] B.K. Siesjö, Pathophysiology and treatment of focal cerebral ischemia. Part I: Pathophysiology, J. Neurosurg. 77 (1992) 169–184.
[9] T.O. Grøndahl, J.J. Hablitz, I.A. Langmoen, Depletion of intracellular Ca^{2+} stores or lowering extracellular calcium alters intracellular Ca^{2+} changes during cerebral energy deprivation, Brain Res. 796 (1998) 125–131.
[10] S. Oda, The observation of rolling mouse Nagoya (rol), a new neurological mutant, and its maintenance, Jikken Dobutsu 22 (1973) 281–288.
[11] C.F. Fletcher, A. Tottene, V.A. Lennon, S.M. Wilson, S.J. Dubel, R. Paylor, D.A. Hosford, L. Tessarollo, M.W. McEnery, D. Pietrobon, N.G. Copeland, N.A. Jenkins, Dystonia and cerebellar atrophy in Cacna1a null mice lacking P/Q calcium channel activity, FASEB J. 15 (2001) 1288–1290.
[12] E. Takahashi, $Ca_v2.1$ channelopathies and mouse genetic approaches for investigating $Ca_v2.1$ channel function and dysfunction, in: M. Yamaguchi (Ed.), Calcium Signaling, Nova Science Publishers Inc., New York, 2012, pp. 149–158.
[13] Y. Mori, M. Wakamori, S. Oda, C.F. Fletcher, N. Sekiguchi, E. Mori, N.G. Copeland, N.A. Jenkins, K. Matsushita, Z. Matsuyama, K. Imoto, Reduced voltage sensitivity of activation of P/Q-type calcium channels is associated with the ataxic mouse mutation rolling Nagoya (tg(rol)), J. Neurosci. 20 (2000) 5654–5662.
[14] C.F. Fletcher, C.M. Lutz, T.N. O'Sullivan, J.D. Jr Shaughnessy, R. Hawkes, W.N. Frankel, N.G. Copeland, N.A. Jenkins, Absence epilepsy in tottering mutant mice is associated with calcium channel defects, Cell 87 (1996) 607–617.
[15] K. Matsushita, M. Wakamori, I.J. Rhyu, T. Arii, S. Oda, Y. Mori, K. Imoto, Bidirectional alterations in cerebellar synaptic transmission of tottering and rolling Ca^{2+} channel mutant mice, J. Neurosci. 22 (2002) 4388–4398.
[16] N.M. Lorenzon, C.M. Lutz, W.N. Frankel, K.G. Beam, Altered calcium channel currents in Purkinje cells of the neurological mutant mouse leaner, J. Neurosci. 18 (1998) 4482–4489.
[17] Y. Sakuraoka, T. Sawada, T. Shiraki, K. Park, Y. Sakurai, N. Tomosugi, K. Kubota, Analysis of hepcidin expression: *in situ* hybridization and quantitative polymerase chain reaction from paraffin sections, World J. Gastroenterol. 18 (2012) 3727–3731.
[18] E. Takahashi, K. Niimi, Spatial learning deficit bon aged heterozygous Cav2.1 channel mutant mice, *rolling* mouse Nagoya, Exp. Gerontol. 44 (2009) 274–279.
[19] A. Mdzinarishvili, W.J. Geldenhuys, T.J. Abbruscato, U. Bickel, J. Klein, C.J. Van der Schyf, NGP1-01, a lipophilic polycyclic cage amine, is neuroprotective in focal ischemia, Neurosci. Lett. 383 (2005) 49–53.
[20] K.O. Cho, Y.S. Kim, Y.J. Cho, S.Y. Kim, Upregulation of DSCR1 (RCAN1 or Adapt78) in the peri-infarct cortex after experimental stroke, Exp. Neurol. 212 (2008) 85–92.
[21] H. Toriyama, L. Wang, H. Saegusa, S. Zong, M. Osanai, T. Murakoshi, T. Noda, K. Ohno, T. Tanabe, Role of $Ca_V2.3$ (alpha1E) Ca^{2+} channel in ischemic neuronal injury, Neuroreport 13 (2002) 261–265.
[22] H. Saegusa, Y. Matsuda, T. Tanabe, Effects of ablation of N- and R-type calcium channels on pain transmission, Neurosci. Res. 43 (2002) 1–7.
[23] K. Jun, E.S. Piedras-Renteria, S.M. Smith, D.B. Wheeler, S.B. Lee, T.G. Lee, H. Chin, M.E. Adams, R.H. Scheller, R.W. Tsien, H.S. Shin, Ablation of P/Q-type Ca^{2+} channel currents, altered synaptic transmission and progressive ataxia in mice lacking the α_{1A}-subunit, Proc. Natl. Acad. Sci. USA 96 (1999) 15245–15250.
[24] T. Turner, M.E. Adams, K. Dunlap, Calcium channels coupled to glutamate release identified by ω-Aga-IVA, Science 258 (1992) 310–313.
[25] T.J. Turner, K. Dunlap, Pharmacological characterization of presynaptic calcium channels using subsecond biochemical measurements of synaptosomal neurosecretion, Neuropharmacology 34 (1995) 1469–1478.
[26] D. Attwell, B. Barbour, M. Szatkowski, Non-vesicular release of neurotransmitter, Neuron 11 (1993) 401–407.
[27] T. Gemba, T. Oshima, M. Ninomiya, Glutamate efflux via the reversal of the sodium-dependent glutamate transporter caused by glycolytic inhibition in rat cultured astrocytes, Neuroscience 63 (1994) 789–795.
[28] D.W. Choi, Glutamate neurotoxicity and diseases of the nervous system, Neuron 1 (1988) 623–634.
[29] H. Kadotani, S. Namura, G. Katsuura, T. Terashima, H. Kikuchi, Attenuation of focal cerebral infarct in mice lacking NMDA receptor subunit NR2C, Neuroreport 9 (1998) 471–475.
[30] D.B. Wheeler, A. Randall, R.W. Tsien, Roles of N-type and Q-type Ca^{2+} channels in supporting hippocampal synaptic transmission, Science 264 (1994) 107–111.